Progress In Electromagnetics Research B, Vol. 53, 107–125, 2013

ONE-DIMENSIONAL PHOTONIC CRYSTAL SELECTIVE FILTERS DESIGN USING SIMULATED ANNEALING OPTIMIZATION TECHNIQUE

Hadjira A. Badaoui[1, *] and Mehadji Abri[2]

[1]Laboratoire STIC, Département de Télécommunications, Faculté des Sciences de l'Ingénieur, Université Abou-BekrBelkaïd-Tlemcen, BP 230, Pôle Chetouane, Tlemcen 13000, Algeria

[2]Laboratoire de Télécommunications, Département de Télécommunications, Faculté des Sciences de l'Ingénieur, Université Abou-BekrBelkaïd-Tlemcen, BP 230, Pôle Chetouane, Tlemcen 13000, Algeria

Abstract—During the last decade, selective photonic crystal filters have received much research interest in the fields of nanotechnology and optical interconnection network. The main focus of this paper consists of an analysis and a synthesis of one-dimensional photonic crystal selective filters. The optimization is performed by employing the simulated annealing algorithm. The filters synthesis is obtained by acting on the Bragg grating layer widths. Simulated annealing is applied to solve the PhC-1D filters synthesis problem in order to reduce the quadratic error and to obtain a desired transmission according to a Gaussian function defined in advance by the user. Starting from the Maxwell's equations for dielectric nonmagnetic structure, we show the derivation of the Helmholtz equation and find its solution for 1D layered structure. In addition, the boundary conditions and equation transformation to set of linear equations which are solved using Cramer's method are described thoroughly. This mathematical technique is then applied for computation of the transmission spectra of 1D perfectly periodic structure and structures with different defects. These results can be easily applied for design of selective filters.

Received 25 May 2013, Accepted 6 July 2013, Scheduled 11 July 2013

* Corresponding author: Hadjira Abri Badaoui (elnbh@yahoo.fr).

1. INTRODUCTION

Photonic crystals (PhCs) are a novel class of optical represented by natural or artificial structures with periodic modulation of the refractive index. Such optical media have some peculiar properties which gives an opportunity for a number of applications to be implemented on their basis. Depending on geometry of the structure PhCs can be divided into three broad categories, namely one-dimensional (1D), two-dimensional (2D) [1] and three-dimensional (3D) structures. Possible applications of photonic crystals are numerous. We can mention a few. A photonic crystal can be very good waveguide, a filter or a prefect mirror. It can also serve as the main material for future devices the same way that semiconductor does for classical computers. Ideally it could help design a laser with a very low threshold [2–5].

The most important property which determines practical significance of the PhC is the presence of the photonic band gap. The photonic band gap (PBG) refers to the energy or frequency range where the light propagation is prohibited inside the PhC. When the radiation with frequency inside the PBG incidents the structure, it appears to be completed reflected. However, if one introduces the defect to the strictly periodic structure, the effect of such a defect is the same as the defect introduction to the crystalline structure of a semiconductor. The means that a new eigen-state appears inside the PBG with energy corresponding to the eigen frequency of the defect. Thus the radiation within the defect frequency will propagate inside the structure or in case of multiple defects radiation will be guided like in waveguide. Thus there exists quite strong analogy between PhC physics and solid-state physics both from the physical and mathematical points of view.

In 1D PhCs "Bragg grating", the periodic modulation of permittivity occurs in one direction only, while in two other directions structure is uniform. It have very low number of possible periodic structure variations because it is represented by the layered structure, so only the refractive index layers thickness and the number of layers within the period can be varied.

It is widely used as a distributed reflector in vertical cavity surface emitting lasers. Besides, such structures are widely used anti reflecting coatings which allow decreasing dramatically the reflectance from the surface and are usd to improve the quality of lenses, prisms and other optical components.

Recently, band-pass photonic crystal filters have attracted great attention due to their important applications in ultrahigh speed information processing. If the signal containing a number of the

wavelength channels falls at the Bragg reflector with defect, only one channel will pass through while others will be reflected.

Filters design is a complicated task, and two essential methods do that. One is based on the PBG analysis and the other by using an optimization technique [6–8].

To achieve this goal, we developed a synthesis method of these PhCs filters by employing an optimization method based simulated annealing (SA). The literature has reported the application of SA for general electromagnetic problems [9–12].

Various synthesis results for one-dimensional photonic crystal selective filters are presented and discussed.

2. SYNTHESIS PROBLEM OF ONE-DIMENSIONAL (1D) PHOTONIC CRYSTAL

In order to start the computation of the 1D structure characteristics, first it is necessary to derive the wave equation from the system of Maxwell's equations.

We consider the corresponding Maxwell's Equations (1) and (2). The material equations for non-magnetic medium take the following form:

$$B(r,t) = \mu_0 H(r,t) \tag{1}$$

$$D(r,t) = \varepsilon_r(r)\varepsilon_0 E(r,t) \tag{2}$$

where μ_0 is the vacuum permeability, and ε_r and ε_0 are the relative permittivity and electric constant.

The Helmholtz equation in given by the following form:

$$\nabla^2 E_0(r) + \varepsilon_r(r)\frac{\omega^2}{c^2}E_0(r) = 0 \tag{3}$$

where ω is the radiation angular frequency.

The Helmholtz equation does not contain time-dependent functions. By solving this equation, it is possible to find the reflectance and transmittance of the finite structure, as well as the field distribution and eigen-frequencies of an infinite structure.

Let us now consider a finite 1D layered structure. The description of the radiation propagation inside such a structure can be found by the solution of the Helmholtz equation presented in the following form:

$$\frac{\partial^2 E_z(x)}{\partial x^2} + \varepsilon_r(x)\frac{\omega^2}{c^2}E_z(x) = 0 \tag{4}$$

Here, we have the coordinate derivative along one direction only because the variation of the permittivity takes place along this

direction only. Thus, we consider the case of light propagating perpendicularly to layer-to-layer interface.

After the 1D Helmholtz equation is written down, it is necessary to define the structure and to find out which parameters of this structure will be taken into account and, thus, should be correctly defined. 1D layered structure can be defined by layer thicknesses, their placement and refractive indices.

Figure 1 depicts an example of the definition of 1D arbitrarily layered structure. Each layer has some specific thickness

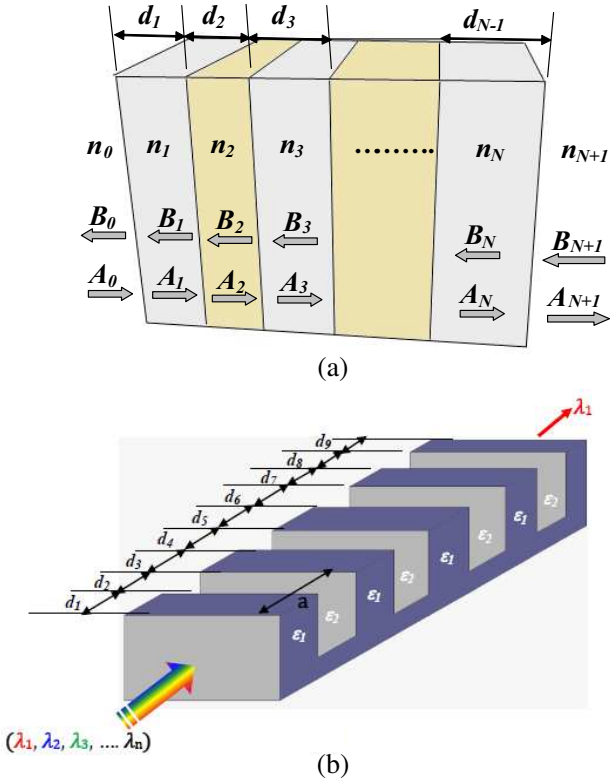

Figure 1. (a) Definition of an arbitrary layered structure. (b) 1D periodic arrangement of nine high and low refractive index layers. The period of the structure is $d_i + d_{i+1}$ $(i = 1 : 8)$. A number of the wavelength channels falls at the Bragg reflector with defect, only one channel will pass through while others will be reflected.

(d_1, d_2, ..., d_{N-1}) and refractive index (n_1, n_2, ..., n_{N-1}).

$$n(x) = \begin{cases} n_1 & 0 \le x \le d_1 \\ n_2 & d_1 \le x \le d_2 \end{cases}$$

With:

$$n(x+d) = n(x), \qquad d = d_1 + d_2$$

The structure is surrounded by material with refractive index $n_0 = n_N$. Arrows indicate forward wave and backward wave inside each layer. Backward waves appear due to the Fresnel reflection from layer-to-layer interface.

After this, it is possible to determine the reflectance and transmittance of the structure. The general solution of the Helmholtz equation for j-th layer takes the following form:

$$E_j(x) = A_j e^{j \cdot n_j \cdot k \cdot x_j} + B_j e^{-j \cdot n_j \cdot k \cdot x_j} \tag{5}$$

where A and B are the amplitudes of forward and backward waves correspondingly.

As for other boundary conditions, they determine the way how the field distribution functions, or wave functions, are "bonded" at the interfaces. In case of 1D layered structure, we consider the tangential component of the electric field only so boundary conditions are formulated as the equality of wave functions and their first derivatives at the interface:

$$E_j(x_j) = E_{j+1}(x_j) \tag{6}$$

$$\frac{\partial}{\partial x} E_j(x_j) = \frac{\partial}{\partial x} E_{j+1}(x_j) \tag{7}$$

where x_j is the coordinate of j-th interface. We now substitute the general solution (10) to the expressions (6), (7) so the resulting system has the following form:

$$\begin{aligned} & A_j e^{j \cdot n_j k x_j} + B_j e^{-j n_j k x_j} = A_{j+1} e^{j \cdot n_{j+1} k x_j} + B_{j+1} e^{-j n_{j+1} k x_j} \\ & j \cdot n_j \cdot k \cdot A_j \cdot e^{j \cdot n_j k x_j} + j \cdot n_j \cdot k \cdot B_j \cdot e^{-j \cdot n_j k x_j} \\ = \; & j \cdot n_{j+1} \cdot k \cdot A_{j+1} \cdot e^{j \cdot n_{j+1} k x_j} - j \cdot n_{j+1} \cdot k \cdot B_{j+1} \cdot e^{-j \cdot n_{j+1} k x_j} \end{aligned}$$

Writing down such an equation system for each structure interfaces; we obtain the system of linear equations containing 2_{N+2}

equations for the structure with N layers. The system contains 2_{N+4} of unknowns:

$$\begin{aligned}
&A_0 e^{i\cdot n_0 k x_0} + B_0 e^{-i n_0 k x_0} = A_1 e^{i\cdot n_1 k x_0} + B_1 e^{-i n_1 k x_0} \\
&i\cdot n_0 \cdot k \cdot A_0 \cdot e^{i\cdot n_0 k x_0} - i\cdot n_0 \cdot k \cdot B_0 \cdot e^{-i\cdot n_0 k x_0} \\
&= i\cdot n_1 \cdot k \cdot A_1 \cdot e^{j\cdot n_1 k x_0} - i\cdot n_1 \cdot k \cdot B_1 \cdot e^{-j\cdot n_1 k x_0} \\
&A_1 e^{i\cdot n_1 k x_1} + B_1 e^{-i n_1 k x_1} = A_2 e^{i\cdot n_2 k x_1} + B_2 e^{-i n_2 k x_1} \\
&i\cdot n_1 \cdot k \cdot A_1 \cdot e^{i\cdot n_1 k x_1} - i\cdot n_1 \cdot k \cdot B_1 \cdot e^{-i\cdot n_1 k x_1} \\
&= i\cdot n_2 k \cdot A_2 \cdot e^{j\cdot n_1 k x_1} - i\cdot n_2 k \cdot B_2 \cdot e^{-j\cdot n_1 k x_1} \\
&A_N e^{i\cdot n_N k x_N} + B_N e^{-i n_N k x_N} \\
&= A_{N+1} e^{i\cdot n_{N+1} k x_N} + B_{N+1} e^{-i n_{N+1} k x_N} \\
&i\cdot n_N \cdot k \cdot A_N \cdot e^{i\cdot n_N k x_N} - i\cdot n_N \cdot k \cdot B_N e^{-i\cdot n_N k x_N} \\
&= i\cdot n_{N+1} \cdot k \cdot A_{N+1} \cdot e^{j\cdot n_{N+1} k x_N} - i\cdot n_{N+1} \cdot k \cdot B_{N+1} \qquad (8)
\end{aligned}$$

In order to solve the system, it is necessary to eliminate two extra variables. For this reason we use the last boundary condition defining the amplitude of the backward wave behind the last layer B_{N+1} to be equal to zero. We also use the initial condition assigning some specific value to the amplitude of the forward wave before the first layer A_0. Obtained linear system of equations is solved by some standard methods such as Cramer's method [13, 14]. As a result of the solution, we have a set of amplitudes of forward and backward waves inside each layer. Let us assume that we have not just an arbitrary, but some finite-size periodic structure; that is, the structure where a group of two or more layers is translated several times. The behavior of such a structure is quite easy to predict if we know its layers' parameters. Such a periodic structure is usually referred to as Bragg grating or distributed Bragg reflector. The peculiarity of the Brag grating is the possibility to fine-tune the transmittance and reflectance spectrum by the variation of layer parameters. At that, the structure has very high reflectance at some specific wavelengths while at another wavelength it may be transparent.

Figure 2 depicts a typical view of the transmission and reflectance spectrum of 1D periodic structure. It is computed by multiple solution of the equation system (8). Each solution is carried out at different wavelengths; hence, the computation gives a number of amplitudes of backward waves B_0 before the first layer of the structure. Dividing this amplitude by the incident wave amplitude A_0 and raising the result to the second power we obtain the reflectance of the structure at each wavelength. As is seen from the Figure 2, the reflectance is quite different at different wavelengths. The reflection wavelength here falls at the wavelength 1.2 μm and 1.75 μm. This means that the maximum of transmission is observed at these wavelengths.

Using the above described method it is possible to design different passive optical devices such as high-efficiency reflectors, anti reflection films, distributed Bragg reflectors for vertical-cavity surface-emitting lasers (VCSEL), wavelength division multiplexers/demultiplexers on the basis of fiber Bragg gratings (FBG), mirrors of tunable lasers, etc..

The synthesis problem consists of approaching the synthesized transmission spectra function of the PhC filter $F_s(\lambda)$ to a Gaussian desired pattern $F_d(\lambda i)$ presented by Equation (9) imposed in advance by the user as shown in Figure 3.

$$F_d(\lambda i) = e^{-\left(\frac{15(\lambda i-\lambda_0)^2}{10^{-2}}\right)} \tag{9}$$

The error made between the two patterns is written:

$$\delta(\lambda,\ d, n) = |F_s(\lambda,\ d, n) - F_d(\lambda,\ d, n)| \tag{10}$$

The optimization problem consists then in minimizing the quadratic error $G(\lambda,\ n)$:

$$G(\lambda) = \sum_{\lambda} \delta^2(\lambda, d, n) \tag{11}$$

The synthesis problem in which we are interested consists of minimizing the quadratic error. The synthesis method used is the simulated annealing algorithm which will be described in detail. SA's have been found to be very effective for the PhCs selective filters optimization, thanks to its robustness and inherent ability to accommodate a variety of constraints.

SA is a probabilistic method based on concepts deriving from statistical mechanics by the means of the famous method of annealing

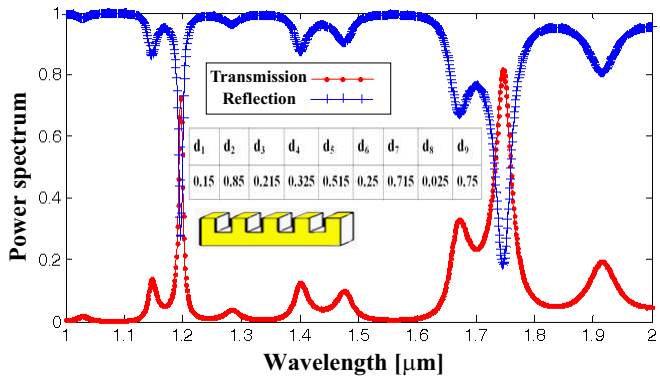

Figure 2. Typical transmission and reflection spectrum of 1D PhC with an arbitrary layer thickness.

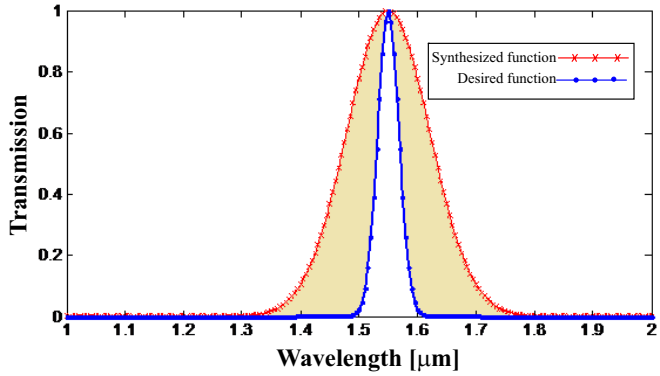

Figure 3. Desired and synthesized function shape pattern specification.

used by the metallurgists. This method uses the Metropolis algorithm [15]. This algorithm is precisely used to randomly draw a continuation from microscopic configurations by respecting the proportions of Boltzmann relating to balance at a given temperature. As for the algorithm of iterative improvement, the algorithm of Metropolis makes it possible to explore by a random walk a graph whose tops are the microscopic configurations of the system.

In the case of the iterative improvement, displacement in the graph is always carried out towards the configurations of decreasing cost, while the algorithm of Metropolis allows sometimes transitions towards configurations from higher cost. In optimization, an iterative research which accepts only the new points corresponding to a lower value of the function is equivalent to a physical system which reaches temperature equal to zero quickly, which brings us at local minima. On the other hand simulated annealing seeks to converge towards the global minimum thanks to the control of the parameter temperature. The algorithm of Metropolis calculates the new function $E_{\text{new}} = f(x_1)$, with x_1 the new point generated starting from a function $g(\Delta x)$, where Δx is the difference between the new point and the current point.

The majority of the optimization methods using simulated annealing choose their new point with variable distances from their starting point or running. If the obtained solution is better than the preceding one, then this solution is accepted. If the preceding solution remains better, a law of probability of acceptance intervenes in order to decide to keep or reject this value

Probability of acceptance determined by a function H, depends on the temperature T and difference between the two values of the

function. As an example, while referring to the Boltzmann law, definite as follows

$$H = \frac{1}{1 + \exp^{(\Delta E/T)}} \approx \exp^{(-\Delta E/T)} \tag{12}$$

where $E = f(x)$ represents the system energy and $\Delta E = E_{\text{new}} - E$ the difference in energy between the new point and the preceding point.

In order to accept or to reject a point for which E_{new} is not better than E, one carries out the lots of a random variable P on $[0, 1]$. If the variable obtained is lower than H the point is then accepted. In the contrary case, the new point is refused. When a new point is accepted, even if the corresponding value of the function is worse than with the preceding point, it becomes then the new point running or solution. At the beginning, the temperature T must be large and a new point must be roughly accepted once on two. With the progression of the algorithm in time, the temperature T is reduced, implying a fall of the acceptance probability of the points. In fact, the value called "temperature" T is only one parameter making, it possible to control the amplitude of the movements and makes it possible to avoid the minima.

When the temperature is null, the probability of transition becomes unit. If energy decreases at the time of the transformation, and that it is null in the opposite case: the algorithm of Metropolis is then identical to an algorithm of iterative improvement, in this case, one is likely to finish trapped in local minima. On the other hand, when the temperature is not null, the algorithm can choose points with a value of the higher function, which makes it possible to avoid the minima in favour of global minima good located in the workspace.

Simulated annealing algorithms are expected to arrive at a good solution only in a statistical sense as in principle an infinitely large number of iterations are necessary to attain the global minimum. In practice to be useful, an acceptable solution must be attained in a finite reasonable number of iterations. For this to be possible, the cooling schedule must be carefully chosen so that the temperature falls only as fast as is compatible with maintaining a quasi equilibrium, otherwise the algorithm will lock in a secondary minimum.

Various cooling schedules have been experimented with (step by step, linear, geometric and exponential) and, as expected, it is important to cool slowly, particularly at low temperatures. Finally, for the tests described here, the modified exponential cooling schedule recommended by Rees and Ball [16] is adopted. However, if a modified exponential scheduling is chosen, almost all process running give slightly different results in term of energy and weight values. This

means that the resulting configuration is stable and close to the optimal one.

We used for the synthesis of our filter transmission the simulated annealing algorithm presented by Corona [17]. This algorithm was tested by various authors and was compared with other techniques like the simplex or gradient conjugate known of the functions comprising local minima. It proved that it always found the global minima which are not the case of the other methods. The algorithm is very simple and is presented in the following general form as shown in Figure A1 displayed in the appendix.

In this section, we focus on the optimization and the design of one-dimensional photonic crystal selective filters by entering proper optimization in order to reduce the quadratic error and to obtain a desired transmission according to a Gaussian function defined in advance by the user.

3. SYNTHESIS RESULTS

In this section, we focus on the optimization of the PhCs in order to obtain a selective filter function. We need to specify wavelength range within which filters will be working. We chose to use a range in length from between 1 µm and 2 µm, and then it is sufficient to start the operation simulation using MATLAB software and scan the frequency range. In these structures we take the following wavelengths 1.1 µm, 1.2 µm, 1.3 µm, 1.4 µm, 1.55 µm, 1.65 µm, 1.75 µm, 1.85 µm and 1.95 µm. The filter must present a maximum of transmission at these wavelengths.

In order to test performances of the proposed approach, we considered a photonic crystal which consists of two layers with following specification: The dielectric material has a dielectric constant of 12.25 (that is, refractive index of 3.5, which corresponds to the effective refractive index in a silicon S_i structure) and an air layer with dielectric constant of 1.

In all the simulations, the SA parameters are set as: $T_0 = 2$, $r_t = 0.1$, $\varepsilon = 10^{-18}$, $X_0 = 10^3$, $v_0 = 10^4$, $Ns = 100$; $Nt = 100$.

The synthesized and the desired function are shown in Figure 4 (a). A plot of the error evolution versus iterations is shown in Figure 4(b).

According to Figure 4(a), there is a transmission in the range [1.05 µm–1.15 µm]. The maximum value is around 100%, obtained at the wavelength 1.1 µm. It is obvious, that the SA curve converge toward the desired function in 4092 iteration, the corresponding error is of about 0.43. A pick of transmission occurred at the wavelength 1.18 µm with a weak value. In general, the result is

acceptable. In the figure below, we present the optimization result of another filter with must resonate at wavelength 1.2 µm. We keep the same SA parameters. A plot of the error evolution versus iterations is shown in Figure 5(b).

According to the figure above, one notice that the algorithm converges at the end of 4477 iterations with an error of about 0.9208. The total transmission is 100% at the desired wavelength. Is is obviously that the result is best in this example because its response is less noise in the rest of the range of wavelengths. Let us take another example; in this case the desired wavelength is fixed 1.3 µm. The simulation result using the SA algorithm of the obtained transmission and the error evolution versus iterations are presented respectively in

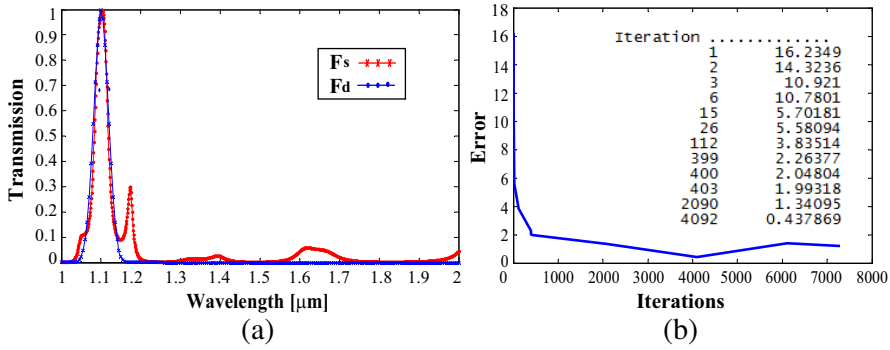

Figure 4. (a) Power transmission spectra for the PhC-1D filter operating at the wavelength 1.1 µm. (b) Error versus iterations.

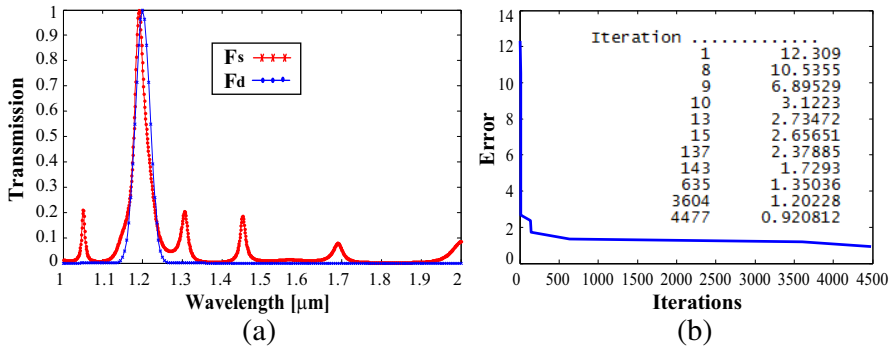

Figure 5. (a) Power transmission spectra for the PhC-1D filter operating at the wavelength 1.2 µm. (b) Error versus iterations.

the Figure 6.

According to the figure Figure 6, one notice that the algorithm converges at the end of 6837 iterations. For the same reason and to test the SA performances, another example is examined. The desired wavelength is set 1.4 µm. The transmission spectra versus wavelength are presented in Figure 7(a) and the error evolution versus iterations are presented respectively in the Figure 7(b).

The algorithm provides a good response after optimization despite some picks less than 30%. The maximum transmission recorded at the wavelength 1.4 µm. The SA converges at the end of 8949 iterations.

Let us now examine the convergence of the SA algorithm at wavelength 1.55 µm. The SA parameters are kept as in the previous

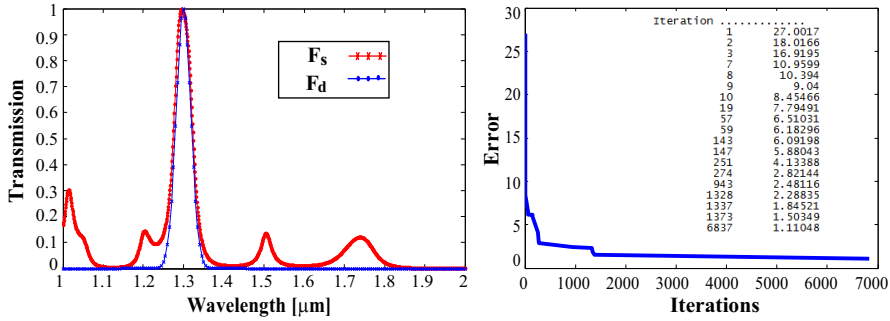

Figure 6. Power transmission spectra for the PhC-1D filter operating at the wavelength 1.3 µm. (b) Error versus iterations.

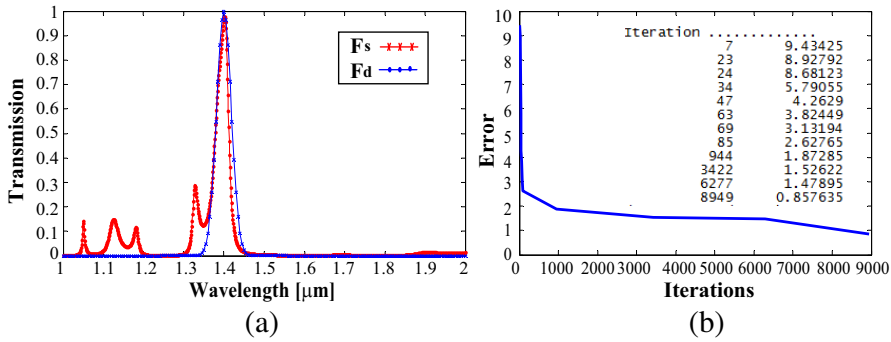

Figure 7. Power transmission spectra for the PhC-1D filter operating at the wavelength 1.4 µm. (b) Error versus iterations.

examples. The obtained results are shown in Figure 8.

Also for this example, the SA converges toward the desired function and the synthesized function takes the form of the desired one after 2041 iteration. A function of filter is realized after this operation. Here we set the desired function presented by a Gaussian at the wavelength 1.65 µm as shown in Figure 9(a). The SA converges toward the desired function with a total transmission of about 100%. The error recorded is of about 0.8471 after 5286 iteration.

According to Figure 10, one notice that the algorithm converges for a centered wavelength 1.75 µm at the end of 9047 iterations. At the rest of frequencies the transmission is null.

Let us now continue with rest of wavelength, here we choose the

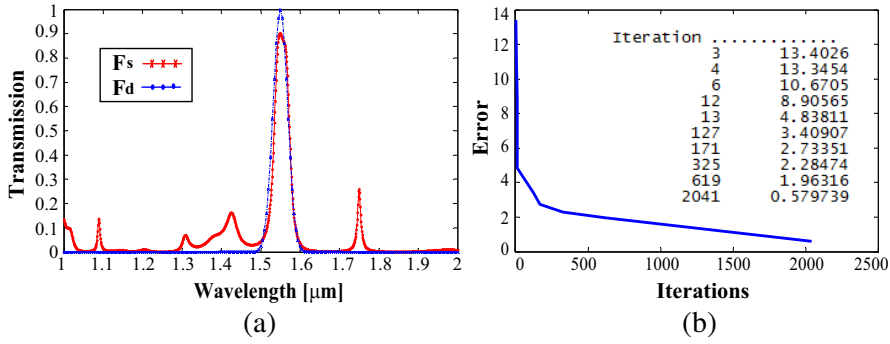

Figure 8. (a) Power transmission spectra for the PhC-1D filter operating at the wavelength 1.55 µm. (b) Error versus iterations.

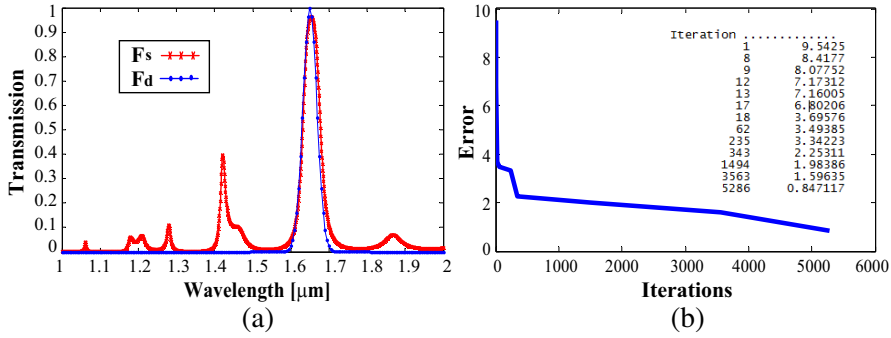

Figure 9. Power transmission spectra for the PhC-1D filter operating at the wavelength 1.65 µm. (b) Error versus iterations.

wavelength 1.85 µm. For this wavelength, the simulated annealing in response offers a solution that may be regarded as perfect as shown in Figure 11(a), since the graph overlaps with that of the desired function. It is obvious from Figure 11(b); that the SA algorithm converges at the end of 6849 iterations.

The last example treated here is for the wavelength 1.95 µm. the Gaussian function is adjusted in order to present a pick at the wavelength 1.95 µm. We keep the same SA parameters. A plot of power transmission spectra for the PhC-1D filter and the error evolution versus iterations is shown in Figure 12. According to the Figure above, one notice that the algorithm converges at the end of 4168 iterations.

In Table 1, we give the corresponding layer widths after optimization for the all the filters.

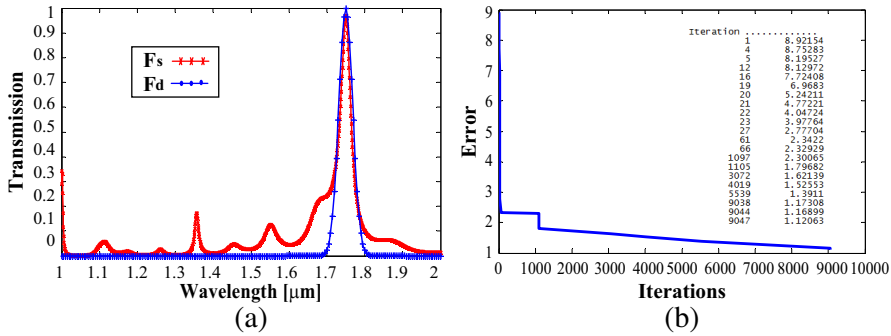

Figure 10. Power transmission spectra for the PhC-1D filter operating at the wavelength 1.75 µm. (b) Error versus iterations.

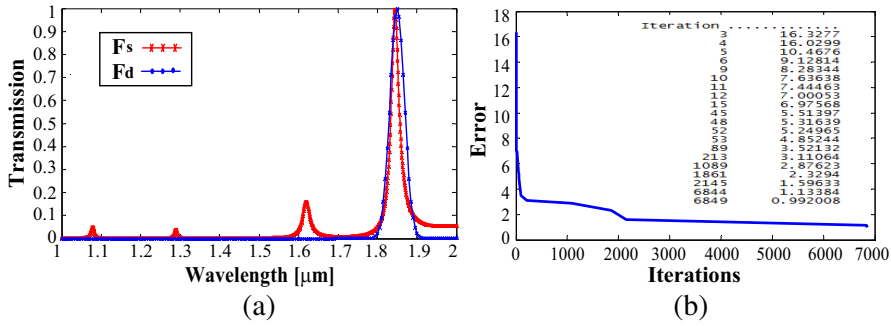

Figure 11. Power transmission spectra for the PhC-1D filter operating at the wavelength 1.85 µm. (b) Error versus iterations.

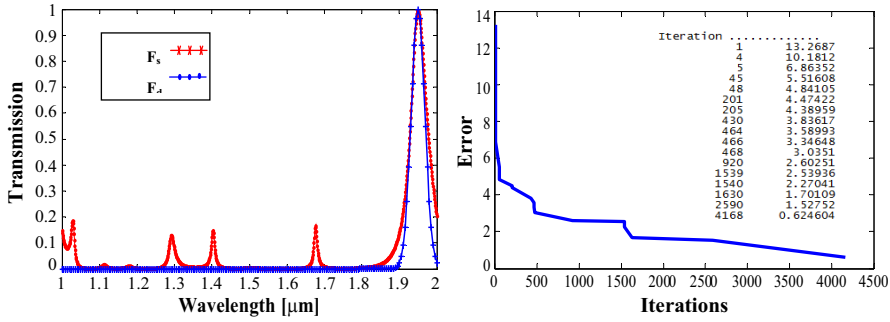

(a) (b)

Figure 12. Power transmission spectra for the PhC-1D filter operating at the wavelength 1.95 μm. (b) Error versus iterations.

Table 1. Corresponding optimized layer widths of different filters.

	Refractive index	n_1	n_2	n_3	n_4	n_5	n_6	n_7	n_8	n_9
		3.5	1	3.5	1	3.5	1	3.5	1	3.5
Wavelengths		d_1	d_2	d_3	d_4	d_5	d_6	d_7	d_8	d_9
	1.10 μm	0.682	0.736	0.544	0.213	0.865	0.693	0.783	0.444	0.811
	1.20 μm	0.305	0.676	0.0604	0.791	0.542	0.160	0.396	0.855	0.056
	1.30 μm	0.811	0.892	0.857	0.263	0.567	0.942	0.318	0.103	0.247
	1.40 μm	0.172	0.196	0.847	0.888	0.255	0.884	0.257	0.437	0.900
	1.55 μm	0.398	0.581	0.300	0.846	0.637	0.208	0.025	0.822	0.944
	1.65 μm	0.567	0.377	0.113	0.824	0.190	0.511	0.418	0.790	0.074
	1.75 μm	0.272	0.236	0.354	0.719	0.417	0.878	0.361	0.387	0.591
	1.85 μm	0.269	0.992	0.458	0.635	0.660	0.054	0.042	0.277	0.074
	1.95 μm	0.298	0.653	0.979	0.701	0.353	0.740	0.295	0.470	0.758

4. CONCLUSION

In this paper, we develop a global optimization algorithm of one-dimensional photonic crystal selective filters based on the simulated annealing method by ordering the distance between layers.

The different cases of filters that we treated, using a synthesis technique based on the simulated annealing algorithm, substantiate

that the application of such an heuristic algorithm achieved the goals of a most rigorous and global approach towards the best solutions. Such solutions remain difficult to achieve using calculus-based on deterministic methods which are too rigid and limited in search space by the local optima difficulties. Moreover, this algorithm is free from all restrictions associated to the integral calculus, derivatives, matrix algebra, discontinuities, etc..

As a result, selective filters were designed successfully operating in several wavelengths.

APPENDIX A.

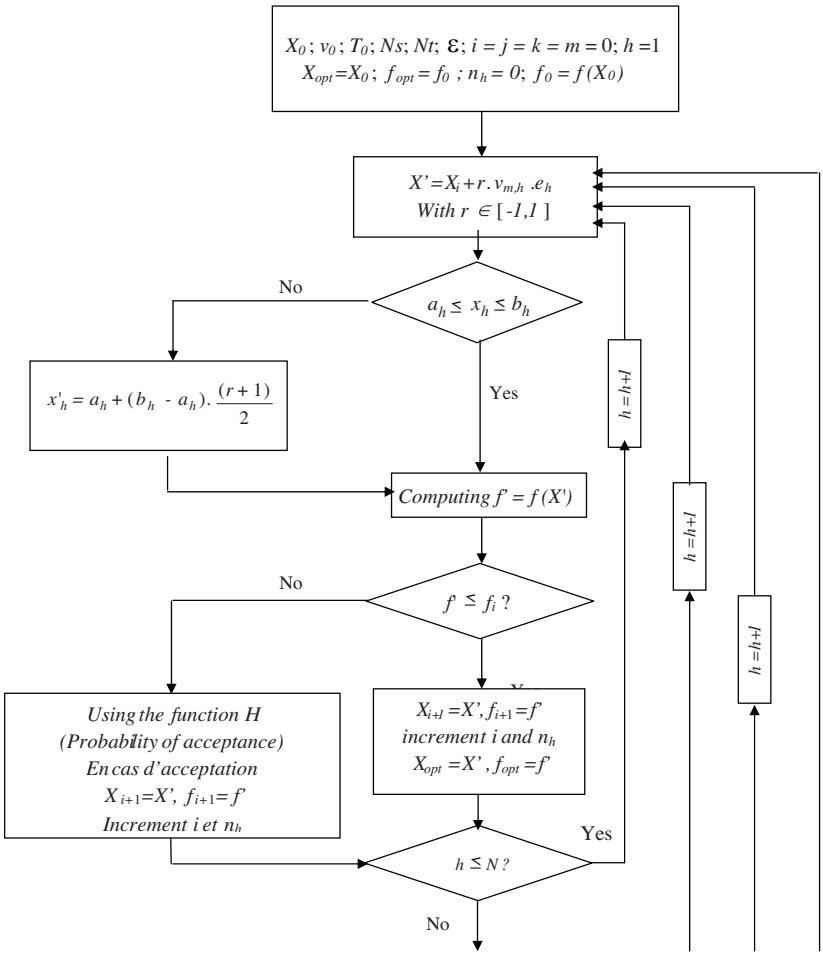

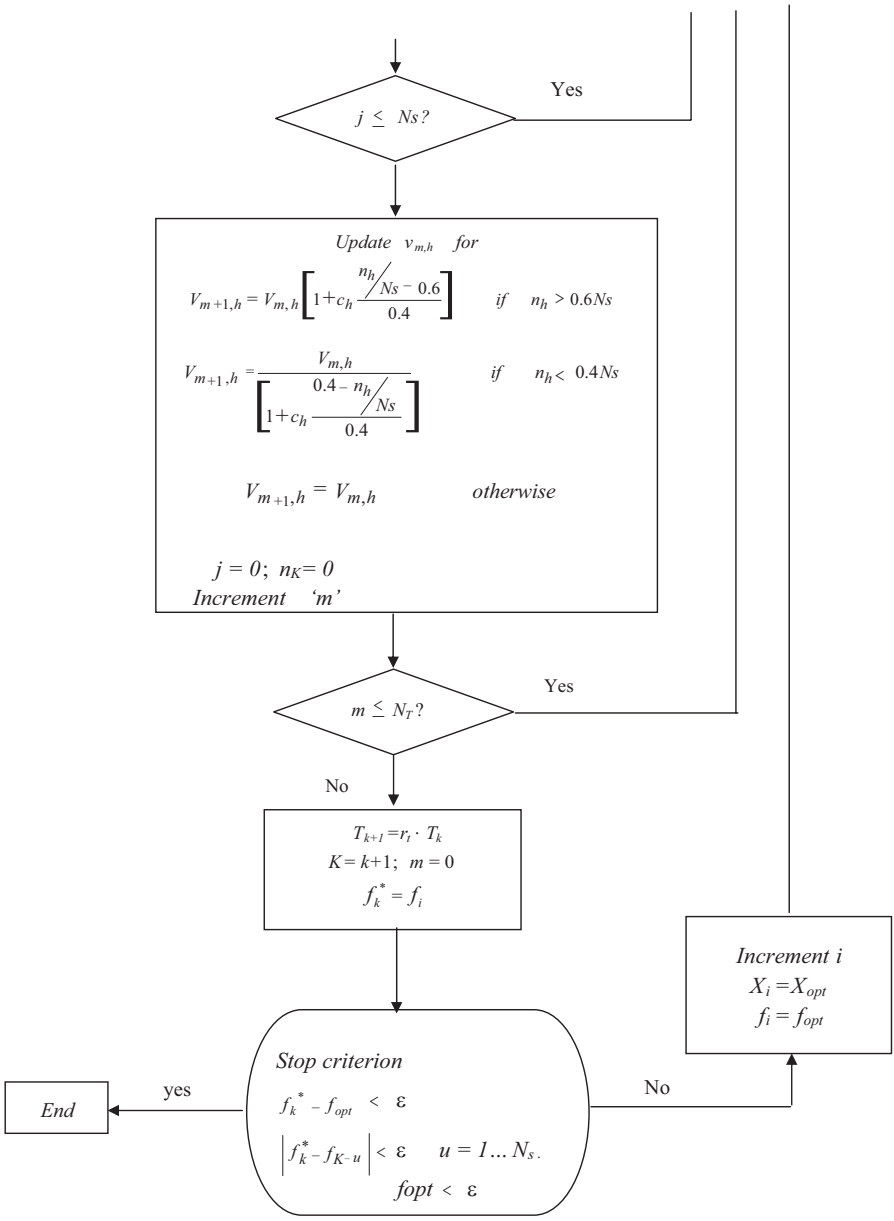

Figure A1. Simulated annealing flow chart process.

REFERENCES

1. Badaoui, H., M. Feham, and M. Abri, "Double bends and Y-shaped splitter design for integrated optics," *Progress In Electromagnetics Research Letters*, Vol. 28, 129–138, 2012.
2. Shambat, G., M. S. Mirotznik, G. Euliss, V. O. Smolski, E. G. Johnson, and R. A. Athal, "Photonic crystal filters for multi-band optical filtering on a monolithic substrate," *Journal of Nanophotonics*, Vol. 3, 031506, 2009.
3. Rumpf, R. C., A. Mehta, P. Srinivasan, and E. G. Johnson, "Design and optimization of space-variant photonic crystal filters," *Appl. Opt.*, Vol. 46, No. 23, 5755–5761, 2007.
4. Solli, D. R., J. J. Morehead, C. F. McCormick, and J. M. Hickmann, "Revisiting photon tunneling through finite 1-D dielectric photonic crystals," *Slow and Fast Light*, Optical Society of America, 2008.
5. Baldycheva, A., V. A. Tolmachev, T. S. Perova, Y. A. Zharova, E. V. Astrova, and K. Berwick, "Silicon photonic crystal filter with ultrawide passband characteristics," *Optics Letters*, Vol. 36, No. 10, 1854–1856, 2011.
6. Awasthi, S. K., U. Malaviya, and S. P. Ojha, "Enhancement of omnidirectional total-reflection wavelength range by using one-dimensional ternary photonic bandgap material," *Journal of the Optical Society of America B*, Vol. 23, 2566–2571, 2006.
7. Preble, S., M. Lipson, and H. Lipson, "Two-dimenisional photonic crystals designed by evolutionary algorithms," *Applied Physics Letters*, Vol. 86, 061111, 2005.
8. Painter, O., JelenaVuckovic, and A. Scherer, "Defect modes of a two-dimensional photonic crystal in an optically thin dielectric slab," *Journal of the Optical Society of America B*, Vol. 16, No. 2, 275–285, February 1999.
9. Muorino, A., C. Trucco, and S. Reggazoni, "Synthesis of unequally spaced arrays by simulated annealing," *IEEE Transactions on Antennas and Propagation*, Vol. 44, 119–122, 1996.
10. Morris, D., "Simulated annealing applied to the misell algorithm for phase retrieval," *IEE Proceedings — Microwaves, Antennas and Propagation*, Vol. 143, 29–38, 1996.
11. Coleman, C. M., E. J. Rothwell, and J. E. Ross, "Investigation of simulated annealing ant-colony optimization, and genetic algorithms for self-structuring antennas," *IEEE Transactions on Antennas and Propagation*, Vol. 52, 100–104, 2004.
12. Abri, M., N. Boukli-hacene, and F. T. Bendimerad, "Ap-

plication du recuit simulé à la synthèse d'antennes en réseau constituées d'éléments annulaires imprimés," *Annales des Télécommunications*, Vol. 60, No. 11, 1420–1438, 2005.

13. Hedman, B. A., "An earlier date for 'Cramer's Rule'," *Historia Mathematica*, Vol. 4, No. 26, 36–368, 1999.
14. Arel, I. and K. Habgood, "A condensation-based application of Crame's rule for solving large-scale linear systems," *Journal of Discrete Algorithms*, Vol. 10, 98–109, 2012.
15. Kirkpatrik, S., C. D. Gelliatt, M. P. Vecchi, "Optimization by simulated annealing," *Science*, Vol. 220, No. 4598, 372–377, 1983.
16. Rees, S. and R. C. Ball, "Criteria for an optimum simulated annealing schedule for problems of the travelling salesman type," *J. Phy. A.: Math. Gen.*, Vol. 20, 1239, 1987.
17. Corana, A., M. Marchesi, C. Martini, and S. Ridella, "Minimising multimodal functions of continuous variables with the 'simulated annealing' algorithm," *ACM Transactions on Mathematical Software*, Vol. 13, 262–280, 1987.